Research Article | Vol. 24, No. 15 | 25 Jul 2016 | OPTICS EXPRESS 16732

Optics EXPRESS

Programmable eye-opener lattice filter for multi-channel dispersion compensation using an integrated compact low-loss silicon nitride platform

RENAN MOREIRA,[1,2,*] SARAT GUNDAVARAPU,[1] AND DANIEL J. BLUMENTHAL[1]

[1]*Electrcial and Computer Engineering Department, University of California, Santa Barbara California 93106, USA*
[2]*now at Freedom Photonics LLC. 41 Aero Camino. Santa Barbara, CA 93117, USA*
[*]*rmoreira@ece.ucsb.edu*

Abstract: A tunable eye-opening lattice filter for dispersion compensation is demonstrated on an ultra low-loss waveguide platform based on a compact high-aspect ratio Si_3N_4 core. A programmable 10th order lattice filter is demonstrated by cascading a total of 21 Mach-Zehnder interferometers with programmable delay lines of lengths designed at the baseband data rate. The filter has a footprint of 2.23 cm^2 with continuously tunable dispersion from −500 ps/nm to 500 ps/nm. The filter shows a periodic transfer function with a measured FSR of 100 GHz capable of compensating multiple WDM channels with a single device.

OCIS codes: (230.7390) Waveguides, planar; (130.0130) Integrated optics; (130.2035) Dispersion compensation devices.

References and links

1. D. Hsu, C. Wei, H. Chen, and J. Chen, "Cost-effective OFDM transmission technologies for long reach PON," in *The Current Trend of Optics and Photonics*, C.-C. Lee (Springer 2015).
2. K. Takiguchi, K. Jinguji, K. Okamoto, and Y. Ohmori, "Variable group-delay dispersion equalizer using lattice-form programmable optical filter on planar lightwave circuit," EEE J. Sel. Top. Quantum Electron. **2**(2), 270–276 (1996).
3. H. Kawashima, N. Matsubara, and K. Nara, "Polarization Insensitive Wideband Tunable Dispersion Compensator with Integrated PLC Type Polarization Diversity Circuit," in Optical Fiber Communication Conference and Exposition and The National Fiber Optic Engineers Conference, Technical Digest (CD) (Optical Society of America, 2006), paper OThE6.
4. F. Horst, R. Germann, U. Bapst, D. Wiesmann, B. J. Offrein, and G. L. Bona, "Compact tunable FIR dispersion compensator in SiON technology," IEEE Photonics Technol. Lett. **15**(11), 1570–1572 (2003).
5. R. Jones, J. Doylend, P. Ebrahimi, S. Ayotte, O. Raday, and O. Cohen, "Silicon photonic tunable optical dispersion compensator," Opt. Express **15**(24), 15836–15841 (2007).
6. S. S. Djordjevic, L. W. Luo, S. Ibrahim, N. K. Fontaine, C. B. Poitras, B. Guan, L. Zhou, K. Okamoto, Z. Ding, M. Lipson, and S. J. B. Yoo, "Fully Reconfigurable Silicon Photonic Lattice Filters With Four Cascaded Unit Cells," IEEE Photonics Technol. Lett. **23**(1), 42–44 (2011).
7. J. F. Bauters, M. J. R. Heck, D. John, D. Dai, M.-C. Tien, J. S. Barton, A. Leinse, R. G. Heideman, D. J. Blumenthal, and J. E. Bowers, "Ultra-low-loss high-aspect-ratio Si3N4 waveguides," Opt. Express **19**(4), 3163–3174 (2011).
8. C. R. Doerr, M. Cappuzzo, A. Wong-Foy, L. Gomez, E. Laskowski, and E. Chen, "Potentially inexpensive 10-Gb/s tunable dispersion compensator with low polarization sensitivity," IEEE Photonics Technol. Lett. **16**(5), 1340–1342 (2004).
9. J. Gehler, R. Wessel, F. Buchali, G. Thielecke, A. Heid, and H. Bülow, "Dynamic Adaptation of a PLC Residual Chromatic Dispersion Compensator at 40Gb/s," in *Optical Fiber Communication Conference, Technical Digest* (Optical Society of America, 2003), paper FN7.
10. L. A. Coldren, S. W. Corzine, and M. L. Mashanovitch, *Diode Lasers and Photonic Integrated Circuits* (Wiley 2012).
11. J. F. Bauters, M. J. R. Heck, D. D. John, J. S. Barton, C. M. Bruinink, A. Leinse, R. G. Heideman, D. J. Blumenthal, and J. E. Bowers, "Planar waveguides with less than 0.1 dB/m propagation loss fabricated with wafer bonding," Opt. Express **19**(24), 24090–24101 (2011).

#266707 http://dx.doi.org/10.1364/OE.24.016732
Journal © 2016 Received 23 May 2016; revised 11 Jul 2016; accepted 12 Jul 2016; published 15 Jul 2016

Optics EXPRESS

12. R. L. Moreira, J. Garcia, W. Li, J. Bauters, J. S. Barton, M. J. R. Heck, J. E. Bowers, and D. J. Blumenthal, "Integrated Ultra-Low-Loss 4-Bit Tunable Delay for Broadband Phased Array Antenna Applications," IEEE Photonics Technol. Lett. **25**(12), 1165–1168 (2013).

1. Introduction

Chromatic dispersion is an undesired fiber characteristic resulting directly from the fact that group delay changes with wavelength. Since a pure single tone signal does not exist, as a pulse propagates along a fiber, different wavelength components will travel at different velocities thus resulting in pulse broadening and limiting the data rate and transmission distance. The dispersion tolerance of a transmission system is inversely proportional to the bit rate squared; therefore, doubling the bit rate deteriorates the tolerance 4x making it a serious problem for high-speed communications. As an example, a 40 Gbps system on a single mode fiber has a dispersion tolerance length of 4 km [1].

Integrated optical tunable filters can be of great benefit to dispersion compensation by providing compact approach that is independent of bit rate. and capable of compensating phase and amplitude distortions. If properly designed, optical filters will have a periodic frequency response that allows for simultaneous compensation of multiple WDM channels using a single device. The tunability of such devices provides a great way to dynamically compensate for residual chromatic dispersion which can fluctuate due to temperature changes, path changes in reconfigurable optical networks, as well as end of life device and system characteristics.

Integrated dispersion equalizers have been demonstrated in several platforms including silica planar lightwave circuits [2–4], and silicon photonics [5, 6]. In this paper we present the first integration of a dispersion-compensating filter on the high aspect ratio Si3N4 core first developed in [7]. The platform is capable of providing state-of-the-art waveguide losses at bend radius 10x smaller than silica waveguides. This platform allows for the integration of a lattice filter with large stage number at a small footprint. The integration of a high order lattice filter allows for the mitigation of optical signal-to-noise ratio (OSNR) penalty of the link for a whole bank of wavelength-division multiplexing (WDM) channels at once due to the filter design. Here we demonstrate a 10-stage optical lattice filter with periodic frequency response capable of compensating +/− 500 ps/nm of dispersion for multiple WDM channels simultaneously. The device is integrated on a high-aspect ratio Si_3N_4 waveguide core, where the core geometry determines the overall loss and bending capabilities [7].

2. Filter design

The tunable lattice filter for dispersion equalization is based on a generalized optical finite impulse response (FIR) filter, which is the same filter architecture also demonstrated by Doerr et. al. and Geheler et. al. [8, 9]. The schematic depicting device architecture for the fabricated programmable 10-stage filter is shown in Fig. 1. Although a conventional lattice filter provides a very low-loss passband, every coupler and phase must be tuned in order to achieve an arbitrary transfer function, which becomes impractical when dealing with high order filters. The generalized filter presented here allows for a "single-knob" dispersion control. Although this design does not allow for arbitrary transfer function realization, the filter is optimized for continuous dispersion tuning between its maximum and minimum setting while still maintaining the low-loss passband characteristic of a lattice filter.

Optics EXPRESS

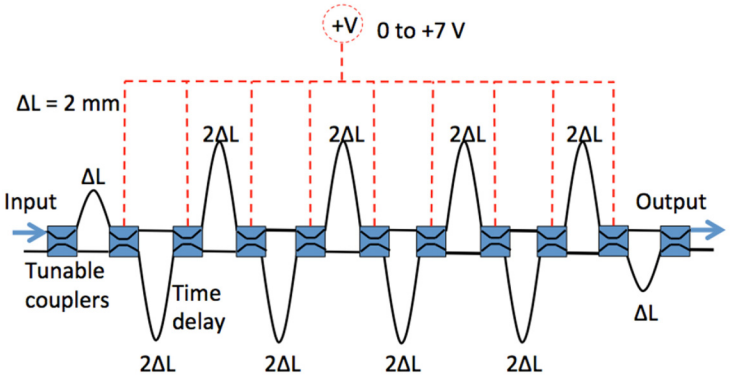

Fig. 1. Schematic of the 10-stage dispersion compensating filter architecture with single knob dispersion control.

The filter is composed of cascaded alternating symmetric and asymmetric Mach-Zehnder interferometers (MZI). Figure 2 shows the breakdown of all the optical elements in a single stage of the optical filter and how each element can be grouped into MZIs accordingly.

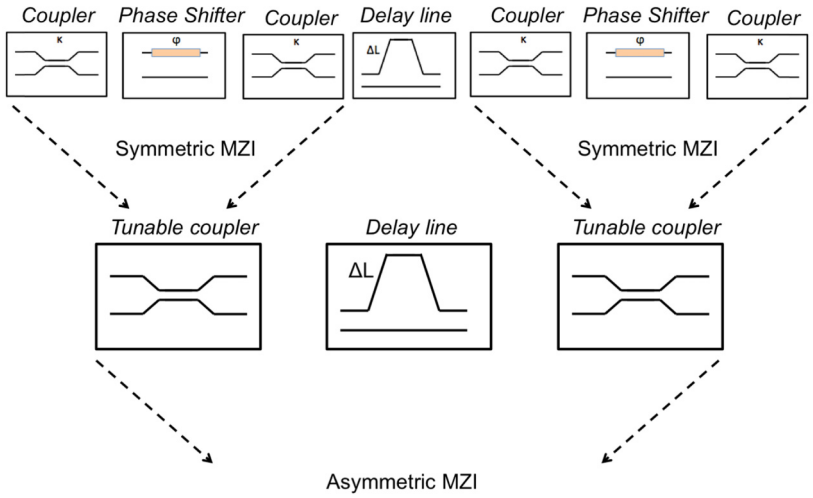

Fig. 2. Schematic of a single stage of the dispersion-compensating filter showing all the building blocks required to describe the filter.

The symmetric MZIs are designed to function as tunable couplers for guiding the path on which the signal will take, while the asymmetric MZIs will mostly function as the dispersive element and set the filter order. It is important to note that the two outer couplers should be set to 0.5 coupling ratio and therefore, when the inner couplers are set to 100/0 (bar state) the entire device will function as a large symmetric interferometer with flat transmission and zero dispersion. As the inner coupling ratio starts to deviate from 100/0, the outer delays act as a mux/demux and all the middle delays act as a long wavelength dependent delay due to the alternating pattern. By controlling the coupling ratio of the inner couplers the device is selecting which paths the “shorter” and “longer” wavelengths will take. The maximum delay is achieved when the couplers are at a 50/50 splitting ratio and outer delays cause the shorter wavelengths to travel along the longest path of the filter.

The time delays are chosen to be an integer multiple of the unit delay, thus making the filter discrete in the time domain. By making the filter discrete in the time domain, this assures the filters periodicity in the frequency domain, which can then be used to

Optics EXPRESS

simultaneously compensate multiple WDM channels. The filter frequency response can then be simulated though the use of a T-matrix formalism, where the main building block is the MZI. The transmission matrix relates the inputs/outputs at a given port to the inputs/outputs at the other, which will allow representation of the device network through a simple matrix multiplication. A single stage MZI consists of two directional couplers with power coupling κ and delay lines of length L_1 and L_2 and can be represented as such.

$$\begin{bmatrix} E_{1out} \\ E_{2out} \end{bmatrix} = \begin{bmatrix} T_{11} & T_{12} \\ T_{21} & T_{22} \end{bmatrix} \cdot \begin{bmatrix} E_{1in} \\ E_{2in} \end{bmatrix} = \mathbf{T} \cdot \begin{bmatrix} E_{1in} \\ E_{2in} \end{bmatrix} \tag{1}$$

Where T is the total transfer matrix for the MZI and can be found by the multiplication of its elements: the first coupler, delay, and second coupler individual transfer matrices [10].

$$\mathbf{T} = \mathbf{T}_{coupler} \cdot \mathbf{T}_{delay} \cdot \mathbf{T}_{coupler} \tag{2}$$

$$T = \begin{bmatrix} \sqrt{1-\kappa} & -j\sqrt{\kappa} \\ -j\sqrt{\kappa} & \sqrt{1-\kappa} \end{bmatrix} \cdot \begin{bmatrix} e^{-jknL_1} & 0 \\ 0 & e^{-jknL_2} \end{bmatrix} \cdot \begin{bmatrix} \sqrt{1-\kappa} & -j\sqrt{\kappa} \\ -j\sqrt{\kappa} & \sqrt{1-\kappa} \end{bmatrix} \tag{3}$$

The κ term is the power coupling coefficient for the coupler, L_1 and L_2 correspond to the MZI delays on each arm, and k is the wave vector equivalent to $2\pi/\lambda$, where λ is the wavelength. With the building block defined cascading the equivalent blocks accordingly can then simulate the entire filter. From the definition in Eq. (1), the T11 matrix element corresponds to the filter transmission from port 1 to port 3 when there is no input in port 2 and so forth. Therefore, the transmission and phase for the filter can be directly extracted from the total T-matrix as described below, and the same can be done to all the matrix elements.

$$Transmission = T_r = \left|T_{11}\right|^2 \tag{4}$$

$$Phase = \Theta = \arg\{T_{11}\} \tag{5}$$

The group delay and dispersion can then be calculated as following:

$$\tau = \frac{d\Theta}{d\nu} \tag{6}$$

$$D = \frac{d\tau}{d\nu} \tag{7}$$

Using the T-matrix approach described above, the filter's response was simulated for different numbers of stages and unit delay length. Figure 3 shows the calculated dispersion amount for the different filter designs. As shown, dispersion is proportional to ΔL^2 for a set number of stages and therefore it is desirable to make ΔL as large as possible. However, the filter passband and free spectral range (FSR) scale with 1/ ΔL and a tradeoff must be considered. Then for a given delay length, the only way to increase dispersion without compromising bandwidth and FSR is by increasing the number of filter stages, which requires a platform with low propagation loss. By using the design curves below, a unit delay length of 2mm was chosen corresponding to an FSR of 100 GHz. As a result, in order to achieve 500 ps/nm of compensation a 10-stage filter is required.

Optics EXPRESS

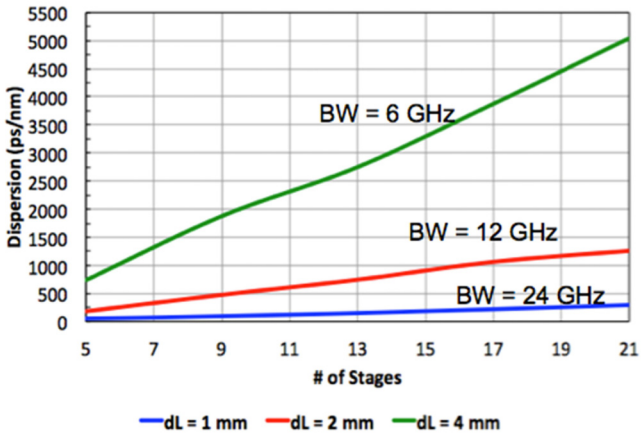

Fig. 3. Simulated filter dispersion for the generalized lattice filter as a function of the number of stages for 3 different unit delay length. The associated bandwidth (BW) is shown above each curve.

3. Waveguide design and fabrication

The tunable dispersion equalizer was fabricated on a high-aspect ratio low-loss silicon nitride waveguide platform as described in [7]. Figure 4 (Left) shows a schematic of the cross-section of the completed waveguide structure. The device was fabricated on a 4" silicon substrate where 15 μm of thermal oxide served as the waveguide lower cladding. Stoichiometric low-pressure chemical vapor deposition (LPCVD) Si_3N_4 was used as the waveguide core and an additional 3 μm of sputtered SiO_2 was deposited as an upper cladding. The device was patterned via 248-nm stepper lithography and etched through reactive ion etching (RIE). The final waveguide structure was then annealed at 1050 °C for 7 hours under N_2 ambient in order to drive out any residual hydrogen impurities from the Si_3N_4 films and/or SiO_2 deposition. The final fabrication step included depositing nickel/chrome and titanium/gold, which served as phase turners via thermo-optic effect and electrical contact, respectively. The metal layers were deposited via e-beam evaporation and patterned through a liftoff process.

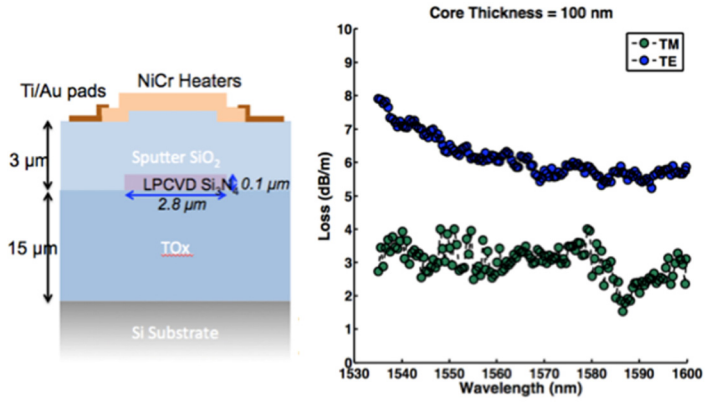

Fig. 4. (Left) Schematic of the fabricated waveguide cross-section. (Right) Measured propagation loss as a function of wavelength for TE and TM polarization.

The waveguide core dimension was 2.8 μm in width by 100 nm in thickness. The core geometry was designed to be single mode at 1550 nm and to provide the aspect ratio required to minimize the optical mode overlap with the sidewall roughness, thus decreasing the

Optics EXPRESS

propagation loss to the low-loss regime. The core thickness of 100 nm was chosen to allow for tight bend radius (500 μm), which is crucial for the smaller footprint, while still maintaining the necessary low propagation loss. Figure 4 (Right) shows the measured TE and TM propagation losses as a function of wavelength over the range from 1530 nm to 1600 nm. The measurement was performed via optical frequency domain reflectometry (OFDR) on a separate 1 meter spiraled waveguide test structure fabricated on the same wafer. The lowest measured waveguide losses were 0.058 dB/cm and 0.018 dB/cm for TE and TM, respectively. Because of the high-aspect ratio of the waveguide geometry, the confinement of the fundamental TM mode is much lower than that of the fundamental TE mode, which in turn results in the measured lower losses. Although the measured TM losses are lower than TE, the minimum bend radius required to keep the bend losses negligible are much higher. Therefore, in order to keep the entire structure footprint small, the device was designed for TE excitation only. A simulated minimum bend radius of 500 μm was required in order to keep the bend losses to < 0.001 dB/cm. At the designed footprint the TM polarization bend losses would be much higher than the overall TE losses and therefore would not operate properly. For the device to be valuable in a system polarization diversity circuit must then be implemented, which is a disadvantage over the square polarization-insensitive doped SiO_2 core PLCs. In contrast, with the measured propagation losses and the simulated bend losses, the platform described here provides a vast advantage over its doped SiO_2 core PLC counterpart, which provides similar propagation losses but at a much higher minimum bend radius of > 5 mm thus placing a limit on the number of stages which can be implemented.

4. Fabrication and measurement results

Figure 5 shows the photo mask layout as well as the actual fabricated device. With the minimum bend radius of 0.5 mm, the device dimensions were 9.89 mm x 22.5 mm, which is equivalent to a footprint of only 2.23 cm^2. The full characterization of the device is broken down into geometry results where we verify the platform's performance (presented in the section above) and then device results, where we look into the filter transmission, group delay, and dispersion. The filter performance on a full transmission link is also evaluated.

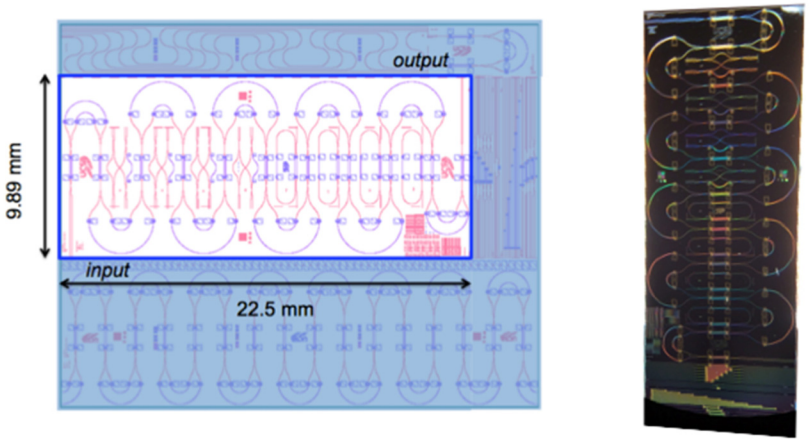

Fig. 5. (Left) Mask layout showing the dimensions for the filter (9.89 mm x 22.5 mm) (Right) Optical microscope picture of the final fabricated device.

4.1 Filter measurement set up

To measure the filter's amplitude response, a CW output from a tunable laser source was sent through a 3-paddle polarization controller and subsequently coupled into the filter via a cleaved fiber. Index matching fluid was used to improve the coupling efficiency and minimize reflections between the fiber and the diced facet. Because the device can only

Optics EXPRESS

support TE mode at the lower loss regime, the optical power was maximized at the output through the use of the polarization controller. The signal transmitted through the device was collected through another cleaved fiber and detected with a broadband photodetector. The laser output power was set to 0 dBm for all of the transmission measurements.

Group delay was measured through OFDR by using a commercially available reflectometer. Because the OFDR technique measures the backscatter signal, a circulator was placed between the device under test (DUT) and the reflectometer as to measure the S_{21} instead of the S_{11}. The amplitude information of the frequency domain data can provide a measure of the device's insertion loss as a function of wavelength, while the phase information of the frequency domain data is used to calculate group delay and chromatic dispersion. By definition, group delay is defined as the rate of change of the phase as a function of wavelength ($\tau = d\phi/d\lambda$), while chromatic dispersion is the rate of change of group delay with respect to wavelength ($D = d\tau/d\lambda$). Both metrics can be calculated directly from the phase information of the OFDR measurements.

4.2 Filter periodicity

The periodicity of the filter response is critical, because it allows for the dispersion compensation of multiple WDM channels through the use of a single device. Therefore, the transmission and group delay response must be periodic throughout the operation of the device. Figure 6 shows the transmission and group delay measurement together with the calculated dispersion for a single bias setting. The filter periodicity can be verified in both results and was measured to be as designed at 100 GHz FSR, as set by the unit delay of 2mm. The figure also shows the filter response for a total of 8 channels, thus making it possible to compensate at least 8 channels simultaneously. The calculated dispersion is shown to be periodic and equivalent on average to −169.7 ps/nm in this case. The dispersion of all 8-channels was measured and a standard deviation of 5.2 ps/nm was calculated indicating that all eight channels were close to the expected value.

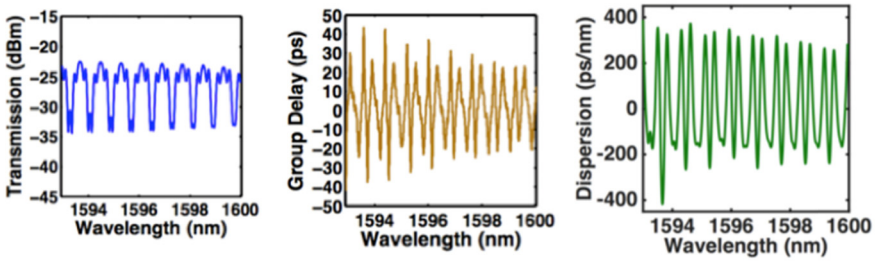

Fig. 6. Measured transmission and group delay for a single bias setting.

The next step was to verify that the filter response could be tuned though the use of the thermo-optic effect without any major change to the periodicity and wavelength grid. Figure 7 below shows the same type of measurements for 4 different biases for the tunable coupler corresponding to an applied voltage of 0, 2, 3.4, and 5.6 V. As the bias setting changes, the coupling ratio at all the couplers varies simultaneously which in turn will change the filter group delay response. As can be seen from the figure, the filter FSR stayed the same for all the bias settings, but the filter transmission and group delay varied with each setting accordingly. Although only 8 channels are demonstrated here, this lattice filter design can be scaled to a larger number of channels provided the wavelength dependence of the directional coupler can be reduced. As the coupling ratio deviates from 3 dB, the filter transmission shape and group delays start to get affected. Small variations in the group delay can be seen in Fig. 6 and Fig. 7 but no degradation of performance was seen on the measure dispersion for each channel.

Optics EXPRESS

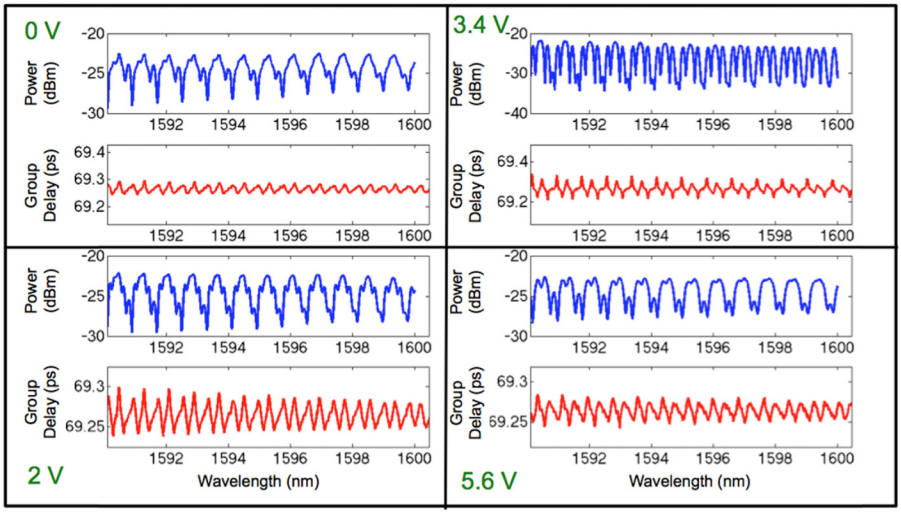

Fig. 7. Filter response for various bias setting on the tunable coupler.

4.3 Insertion loss

It is important to note that transmission data in the previous section was not normalized; and therefore, after we consider the measured setup system losses of 2.0 dB and an input power of 0 dBm, the filter was found to have a total insertion loss of 21.8 dB. The total insertion loss deviates from the optimal loss due to the fabrication process and it is not due to the platform and/or filter design. Although the device becomes unusable for long-haul communications at the current insertion loss value, the device functionality can still be verified. Therefore, if the device is to become useful, the total insertion loss must be properly addressed. By simply moving the phase tuner heaters further away from the waveguide core (at the sacrifice of tuning efficiency) and by introducing waveguide offsets on straight-to-bend transitions the total insertion loss of the device can be dropped to below 4 dB. The loss components are summarized below and can then be broken down into 4 different components that are separately explained in this section: propagation loss, coupling loss, metal absorption loss, and bend loss.

The waveguide propagation loss, as previously stated, was measured to be 0.058 dB/cm. The total propagation length of the device is 20.8 cm; therefore, the waveguide loss contribution to the total insertion loss is only 1.2 dB. The coupling loss was characterized on multiple straight waveguides adjacent to the filter as to minimize the potential of any coupling variation. The coupling loss was measured to be 2.88 ± 0.15 dB/facet, which contributes a total of 5.8 dB to the total insertion loss. Coupling loss on this platform can be further improved through the use of spot-size converter to losses < 1 dB/facet [11]. The third part of the insertion loss corresponded to the metal absorption caused by the heating element being placed too close to the core, 3 μm above the core in this case. To measure the metal absorption, the filter transmission was measured with and without the heaters. Figure 8 shows the filter response with and without metal for a successful measurement of metal absorption of 5.5 dB.

Optics EXPRESS

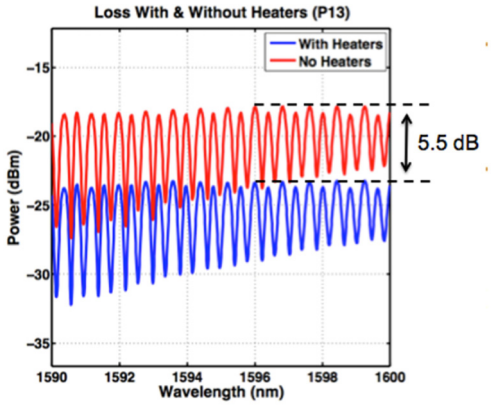

Fig. 8. Filter transmission with heaters and no heater for the same filter, corresponding to a metal absorption loss of 5.5 dB.

The remaining 9.3 dB of insertion loss can then be attributed to bend loss and coupler loss. After further investigation, it was realized that no offsets were placed between the transitions of bent to straight waveguides and between the transitions of two bent waveguides of different direction. The transition mismatch loss was simulated to be 0.04 dB/transition for straight-bend and twice for bend-bend. Although the simulated losses are small, there are a total of 80 straight-straight and 60 s-bends. Therefore, the overall transition bend loss from the simulated values corresponds to 8.6 dB, which almost completely accounts for the remaining insertion loss. Since the mode mismatch between the bend transitions is a dominant cause of loss, the next generation device can resolve this issue by adding waveguide offsets to allow for higher optical mode overlap between transitions.

4.4 Lattice filter tuning and dispersion compensation

To analyze the device's ability to compensate dispersion, we then analyze the filter's full response at a single channel since no major dispersion variance was seen between channels. The device is measured at a total of seven different bias points from 0 to 7 Volts with a maximum power dissipation of 723 mW. The filter's group delay response is controlled by adjusting the coupling ratio of the tunable coupler through the thermo-optic effect by applying current to a single arm of the MZI. The heaters were 10 μm wide and 1000 μm in length, and the response was measured and varied from 0/100 to 100/0, a complete switch characterization is shown in [12]. Figure 9 displays the transmission and group delay response for a single channel for all seven different voltage biases.

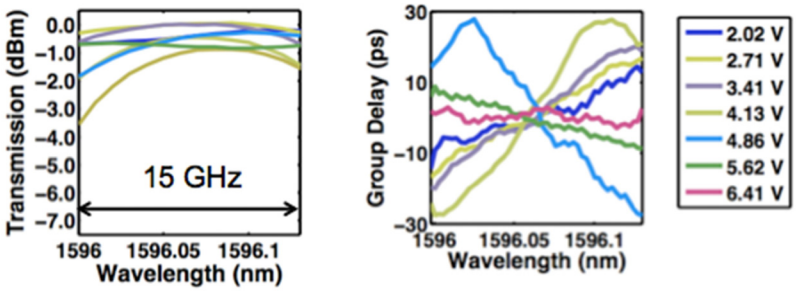

Fig. 9. Complete filter characterization for a single passband, showing transmission and group delay results for seven different bias settings.

The transmission plot (left) data is normalized to the lowest loss transmission in order to highlight the difference in transmission between each bias setting. As can be seen from the

Optics EXPRESS

plot, the transmission remains above 3 dB for all of the bias settings with a measured "useful" bandwidth of 15 GHz. Figure 9 (right), shows a linear group delay across the transmission bandwidth for all the different biases. Because dispersion is defined as the rate of change of group delay over wavelength, a linear group delay response is equivalent to a constant dispersion. Therefore, dispersion can be determined by finding the slope of the group delay by fitting a straight line through the data. The plot also shows different slope signs for various settings, which correspond to the filter's ability in compensating positive and negative dispersion.

An example of the linear fit in order to extract dispersion is shown in Fig. 10 (left). The figure shows a measured dispersion value of 170 ps/nm for that specific setting with a group delay ripple of ± 4 ps. A similar fit can be done for the remaining bias points in order to extract the dispersion value. A summary for all of the measured dispersion as a function of voltage setting is shown in Fig. 10 (right). From the measured results, the filter displays the ability to compensate ± 550 ps/nm with settings between 0 and 7 V.

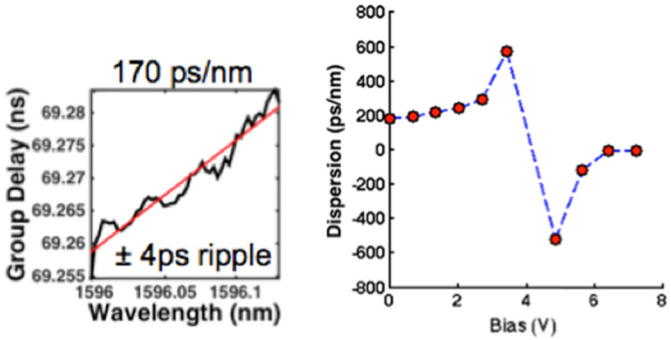

Fig. 10. (Left) Example of a linear fit through a group delay data showing a measured dispersion of 170 ps/nm and a group delay ripple of +/– 4 ps. (Right) Filter measured dispersion as a function of voltage bias.

4.5 Link testing

The final step to verify the filter's functionality is to compensate dispersion of a full transmission link. Transmission measurements were performed on a 40 Gbps NRZ-OOK signal according to the setup in Fig. 11.

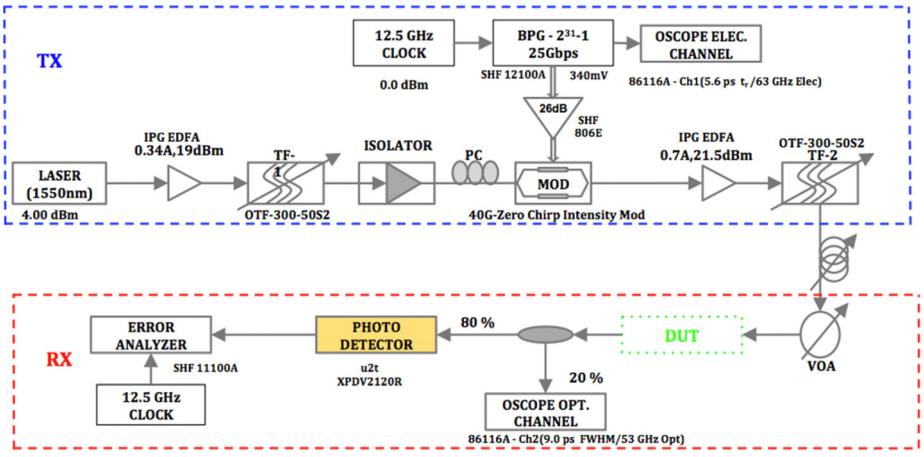

Fig. 11. Dispersion equalizer transmission testbed.

Optics EXPRESS

A 10-kilometer single-mode fiber spool was used to introduce dispersion. For the given fiber length, the calculated dispersion expected is approximately 170 ps/nm. The received data for the uncompensated link shows a distorted and closed eye diagram as seen in Fig. 12 (left). The dispersion equalizer is introduced and biased accordingly to fully compensate the dispersion. Figure 12 (right) shows the compensated detected eye diagram demonstrating the signal improvement over the uncompensated case. The required bias to achieve the eye diagram in Fig. 12 (right) was 98 mA with a corresponding voltage of 7.31V. At this time, only a single channel has been measured. The result then assures, at a first pass, the filter's proper functionally by improving a 40 Gbps signal. To further prove the device complete functionality a full transmission link study at multiple channels must be done including bit error ratio (BER) analysis, which is not included in this paper. This paper focus primarily on device fabrication and response and a system level paper is to be followed. It is important to recall that dispersion tolerance is inversely proportional to bit-rate square, and for a 40 Gbps signal that is equivalent to 4 km of uncompensated propagation on single-mode fiber. Therefore, the filter presented here provides sufficient dispersion compensation for high-speed communications.

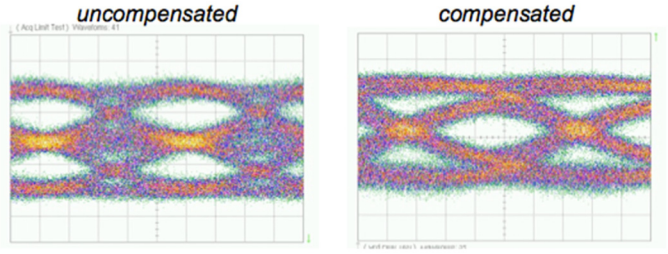

Fig. 12. Eye diagrams for the uncompensated transmission link (left) and compensated link (right).

5. Conclusion

A programmable 10-stage monolithically integrated lattice filter dispersion compensator was demonstrated on an integrated Si_3N_4 waveguide platform that offers superior performance for system loss due to its low waveguide propagation loss. This single device can compensate for a bank of WDM channels on a grid of 100 GHz with a 0.6 dB maximum propagation loss. The platform also provides a tighter bend radius, which directly corresponds with a footprint reduction of more than twice of that of its silica counterparts. The device can compensate +/– 550 ps/nm and dispersion compensation was demonstrated on a 40 Gbps NRZ-OOK signal.

Funding

TE Connectivity, Terabit Optical Ethernet Center (TOEC), DARPA MTO (HR0011-09-C-01233).